SISSA 47/2004/EP
hep-ph/0406328

Update of the Solar Neutrino Oscillation Analysis with the 766 Ty KamLAND Spectrum

Abhijit Bandyopadhyay[1], Sandhya Choubey[2,3], Srubabati Goswami[4], S.T. Petcov[3,2,5], D.P. Roy[6,7]

[1] *Saha Institute of Nuclear Physics, 1/AF, Bidhannagar, Calcutta 700 064, India,*
[2] *INFN, Sezione di Trieste, Trieste, Italy,*
[3] *Scuola Internazionale Superiore di Studi Avanzati, I-34014, Trieste, Italy,*
[4] *Harish-Chandra Research Institute, Chhatnag Road, Jhusi, Allahabad 211 019, India,*
[5] *Institute of Nuclear Research and Nuclear Energy, Bulgarian Academi of Science, Sofia, Bulgaria,*
[6] *The Abdus Salam International Centre for Theoretical Physics, I-34100, Trieste, Italy,*
[7] *Tata Institute of Fundamental Research, Homi Bhabha Road, Mumbai 400 005, India*

Abstract

We investigate the impact of the 766.3 Ty KamLAND spectrum data on the determination of the solar neutrino oscillation parameters. We show that the observed spectrum distortion in the KamLAND experiment firmly establishes Δm^2_{21} to lie in the low-LMA solution region. The high-LMA solution is excluded at more than 4σ by the global solar neutrino and KamLAND spectrum data. The maximal solar neutrino mixing is ruled out at 6σ level. The 3σ allowed region in the $\Delta m^2_{21} - \sin^2\theta_{12}$ plane is found to be remarkably stable with respect to leaving out the data from one of the solar neutrino experiments from the global analysis. We perform a three flavor neutrino oscillation analysis of the global solar neutrino and KamLAND spectrum data as well. The 3σ upper limit on $\sin^2\theta_{13}$ is found to be $\sin^2\theta_{13} < 0.055$. We derive predictions for the CC to NC event rate ratio and day-night (D-N) asymmetry in the CC event rate, measured in the SNO experiment, and for the suppression of the event rate in the BOREXINO and LowNu experiments. Prospective high precision measurements of the solar neutrino oscillation parameters are also discussed.

1 Introduction

The last four years will most likely be described in the future as the golden years of solar neutrino physics. The pioneering results of the Homestake experiment [1], which first observed neutrinos emitted by the Sun and discovered the existence of a solar neutrino deficit [1], and of the Kamiokande [3], SAGE and GALLEX/GNO [4] experiments, which confirmed and extended the Homestake results on the solar neutrino deficit, were reinforced during the last four years by a series of precision measurements by the Super-Kamiokande(SK) [5], SNO [6],[7],[8] and KamLAND [9] experiments. With the recent publication of the KamLAND 766 Ty spectrum data [10] and under the plausible assumption of CPT-symmetry, for the first time a unique solution of the solar neutrino problem in terms of neutrino oscillations [11, 12] can be unambiguously identified. Let us summarize the main steps of the progress in our understanding of the solution of the solar neutrino problem, made in this past four years.

- The first charged current (CC) data from SNO [6] together with absence of distortions of the spectrum of the final state e^- in the $\nu - e^-$ elastic scattering reaction due to solar neutrinos, measured with a high precision in the SK experiment [5], excluded the vacuum oscillation (VO) and the small mixing angle (SMA) MSW [12] solutions in favour of the large mixing angle (LMA) MSW and LOW solutions [13, 14].

- The first neutral current (NC) solar neutrino data from SNO [7], obtained by observing the solar neutrino capture on D_2O (Phase I of the experiment), provided a direct estimate of the Boron neutrino flux normalisation f_B. It confirmed the Standard Solar Model (SSM) prediction for this quantity (the uncertainty in the experimentally determined f_B was smaller than that in the SSM prediction). This implied that the CC rates of Cl, SK and SNO are indeed smaller than 0.5. This strongly favoured the LMA MSW solution over the LOW solution and a non-maximal solar neutrino mixing angle [15].

- The convincing evidence in favour of the LMA solution was obtained in the KamLAND experiment with reactor $\bar{\nu}_e$ [9], which published first results, based on statistics of 162 Ty, in December of 2002. Under the plausible assumption of CPT invariance, the suppression of the reactor $\bar{\nu}_e$ flux observed in the KamLAND experiment firmly established the LMA solution, ruling out the LOW solution at about 5σ level. Moreover, the 162 Ty KamLAND data on the e^+-spectrum distortion, combined with the global solar neutrino data, implied that the LMA solution was confined to two sub-regions : low-LMA (or LMA-I), centered around $\Delta m^2 = 7.2 \times 10^{-5}$ eV^2, and high-LMA (or LMA-II) with Δm^2 centered around $\Delta m^2 = 1.5 \times 10^{-4}$ eV^2. It was found that in both cases $\sin^2\theta \approx 0.3$. The best-fit was in the low-LMA region, while the high-LMA region was allowed only at 99% C.L. [16, 17]

- Finally the NC data from the salt phase of the SNO experiment [8], provided a more precise measurement of f_B. The inclusion of these data in the global solar neutrino oscillation analysis reduced further the allowed region of solar neutrino oscillation parameters. Now

[1] Let us recall that the Cl-Ar method of neutrino detection, used in the Homestake experiment, was first proposed in [2].

the high-LMA region was allowed only at 2.65 σ level, while the maximal solar neutrino mixing was excluded at about 5σ [18, 19].

One of the most important issues after these developments was the definitive resolution of the high-LMA and low-LMA solution ambiguity. This was expected to lead to a precise determination of the neutrino mass squared difference driving the solar neutrino oscillations. For this reason a study of KamLAND 410 Ty and 1000 Ty simulated spectrum data, corresponding to different points in the parameter space, spanning the low-LMA and high-LMA solution regions, was made in [18]. This study showed, in particular, that if the true KamLAND 1000 Ty spectrum data corresponded to a point in the low-LMA region, the high-LMA solution would be ruled out at 3σ level by the combined solar and KamLAND data, while the low-LMA solution region will be considerably reduced. The best-fit point obtained from the analysis of the energy spectrum of the recently released 766.3 Ty data from KamLAND indeed lies inside the low-LMA region [10]. And the combined global solar and KamLAND data indeed excludes the high-LMA solution at 3σ level, in agreement with the above expectation.

In this article we investigate the impact of the 766.3 Ty KamLAND spectrum data on the determination of the solar neutrino oscillation parameters. We perform first a two-neutrino oscillation analysis of the global solar neutrino and the latest KamLAND spectrum data. This permits us to quantify the improvements in the precision of determination of the solar neutrino oscillation parameters which the new KamLAND data imply and, in particular, to assess the status of the high-LMA solution. We check the stability of the allowed region of values of the solar neutrino oscillation parameters thus derived with respect to leaving out from the analysis the data from one of the solar neutrino experiments. This serves also as a check of the consistency between the data from the different experiments and gives some idea about the level of redundancy of the global solar neutrino data set. We next extend the analysis to the case of three neutrino oscillations. We derive, in particular, a new upper limit on the CHOOZ mixing angle θ_{13}, and study the dependence of the allowed values of the parameters Δm^2_{21} and $\sin^2\theta_{12}$ which drive the solar neutrino oscillations, on the value of $\sin^2\theta_{13}$. We give predictions for the CC to NC event rate ratio and day-night (D-N) asymmetry in the CC event rate, measured in the SNO experiment, for the suppression of the event rate in the BOREXINO and LowNu experiments, designed to measure the ^7Be and pp solar neutrino fluxes. Finally, we discuss also how the precision of $\sin^2\theta_{12}$ determination can improve with the increasing of the precision of the future SNO data, as well as, by performing a reactor $\bar{\nu}_e$ oscillation experiment with a baseline ~ 70 km.

2 Two Flavour-Neutrino Oscillation Analysis

We first present the results of a standard two-flavor neutrino oscillation analysis. We use the 13 bin KamLAND spectrum data and define a χ^2 assuming a Poisson distribution as

$$\chi^2_{klspec} = \sum_i \left[2(X_n S^{theory}_{KL,i} - S^{expt}_{KL,i}) + 2S^{expt}_{KL,i} \ln(\frac{S^{expt}_{KL,i}}{X_n S^{theory}_{KL,i}}) \right] + \frac{(X_n - 1)^2}{\sigma^2_{sys}}, \quad (1)$$

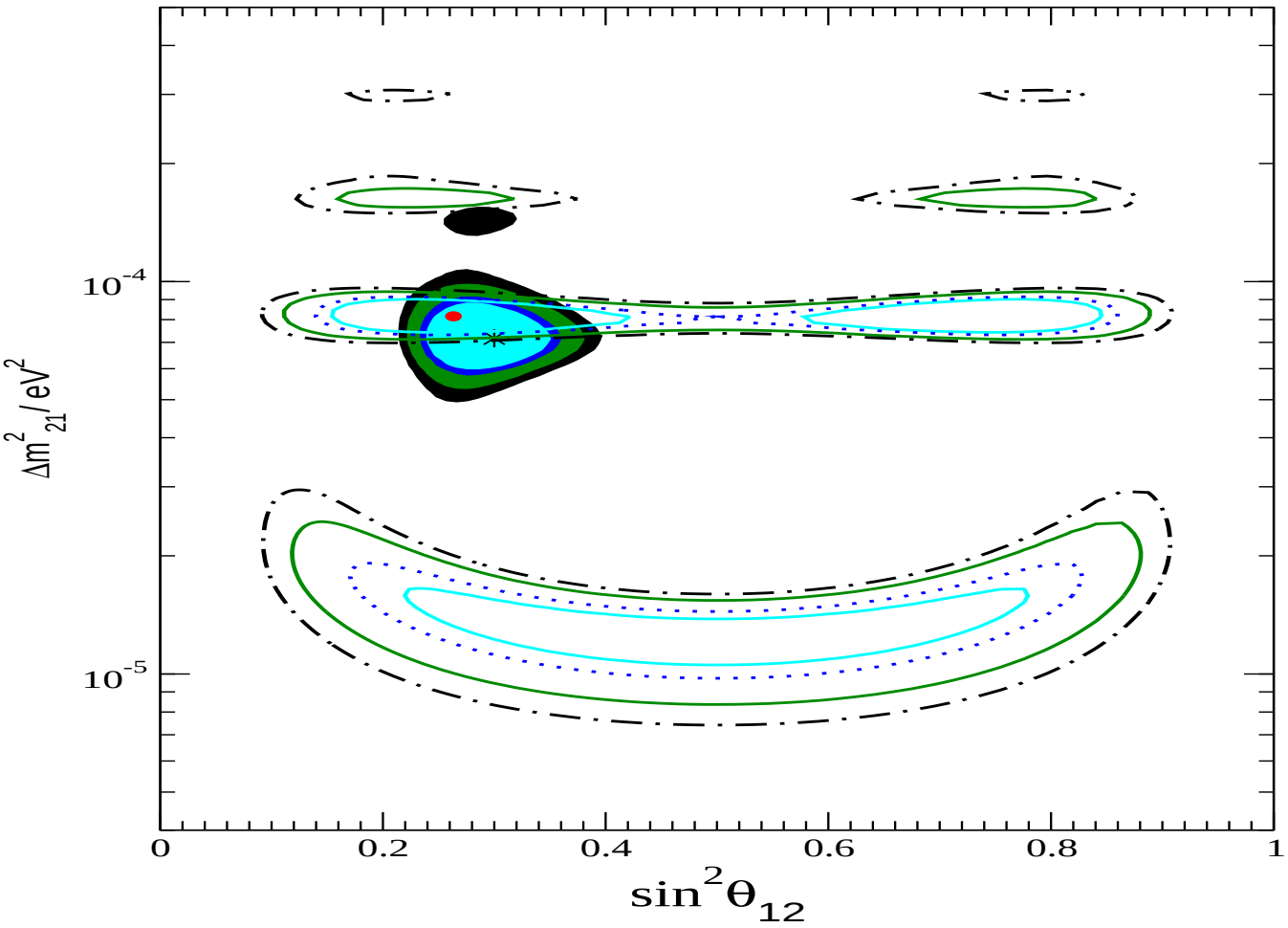

Figure 1: The 90%, 95%, 99% and 99.73% C.L. allowed regions in the Δm^2_{21} $-\sin^2\theta_{12}$ plane from a χ^2-analysis i) of the 766.3 Ty KamLAND data (white areas within contour lines), and ii) of the global solar neutrino and 162 Ty KamLAND data (shaded areas). The best fit points in the two cases are marked by a black dot and by a star, respectively.

where X_n is allowed to vary freely and σ_{sys} is the systematic uncertainty. [2] We include the revised resolution width, fuel composition, detector fiducial mass and efficiencies from [10]. The other details of our analysis can be found in [16, 20]. Some of the reactors, particularly the Kashiwazaki-Kariwa and Fukushima I and II reactor complexes, were partially/totally shut-down during some of the period of data taking in KamLAND. We have approximately taken into account this change in the reactor flux due to the reactor shut-down using the plots showing the time variations of the number of fissions in a given reactor and hence the expected reactor $\bar{\nu}_e$ flux in KamLAND

[2]Note that several theoretical and experimental systematic errors like those due to energy scale, reactor spectrum etc. are energy dependent. However, these details being inacessibile to us, we have used the same total systematic error for all the bins. Detailed information by the KamLAND collaboration on the errors and their correlations in each bin will make our analysis more accurate. As KamLAND statistics is increased and systematics start to dominate more detailed information from the KamLAND collaboration will be an important requirement.

[21]. We have also used the information on the reactor operation schedules available on the web [22]. In the latest version of [10], the KamLAND collaboration have identified a new source of background in the their analysis, coming from $^{13}C(\alpha, n)^{16}O$ reaction induced by the α decay of the radon daughter ^{210}Po in the liquid scintillator. This increases the total background in their $\bar{\nu}_e$ signal to 17.8 ± 7.3 above $E_{vis} = 2.6$ MeV. We include in our analysis, this new background and its associated uncertainty.

We show by the unshaded contours in Fig. 1 the allowed regions obtained using the 766.3 Ty KamLAND spectrum data. The best-fit according to our analysis is at [3]

$$\Delta m^2_{21} = 8.2 \times 10^{-5}\ \text{eV}^2, \quad \sin^2\theta_{12} = 0.26, \quad \chi^2_{min}/d.o.f. = 15.24/10 \tag{2}$$

The best-fit value of Δm^2_{21} we find agrees reasonably well with that obtained by the KamLAND collaboration [10], while our best fit value of $\sin^2\theta_{12}$ is somewhat lower than that found in [10] because of differences in the fitting procedure and the relative insensitivity of the KamLAND data to this parameter. The regions at $\Delta m^2 \geq 2 \times 10^{-4}$ eV^2 which were allowed by the KamLAND 162 Ty spectrum data [9], are now severely disfavored due to increased precision on the observed spectral distortion and only a very tiny area is allowed at the 3σ level. Superposed on the same figure, we show by the shaded areas the allowed regions obtained using the combined solar neutrino + 162Ty KamLAND data. As it follows from this figure, the best-fit point of the new KamLAND spectrum data lies inside the allowed low-LMA region, obtained in the solar neutrino + 162 Ty KamLAND spectrum data analysis.

In Fig. 2 we show the allowed region obtained from the combined analysis of the global solar neutrino data and the 766.3 Ty KamLAND spectrum data. The dashed line in the figure indicates the region allowed at 90% C.L. by the global solar neutrino data alone. The star (dot) marks the best-fit point of the solar neutrino + 766.3 Ty KamLAND (solar neutrino) data. We have used in this analysis the solar neutrino data on the total event rates from the radiochemical experiments Cl [1] and Ga (Gallex, SAGE and GNO combined) [4], the 1496 day 44 bin Zenith angle spectrum data from SK [5], the combined CC, NC and Electron Scattering (ES) 34 bin energy spectrum data from the phase I (pure D_2O phase) of SNO [7] and the data on CC, NC and ES total observed rates from the phase II (salt phase) of the SNO experiment [8].

For the combined analysis of solar and KamLAND data we define the global χ^2 as

$$\chi^2_{global} = \chi^2_{\odot} + \chi^2_{klspec} \tag{3}$$

where

$$\chi^2_{\odot} = \sum_{i,j=1}^{N} (R_i^{\text{expt}} - R_i^{\text{theory}})(\sigma^2_{ij})^{-1}(R_j^{\text{expt}} - R_j^{\text{theory}}) \tag{4}$$

where R_i are the solar data points, N is the number of data points and $(\sigma^2_{ij})^{-1}$ is the inverse of the covariance matrix, containing the squares of the correlated and uncorrelated experimental and

[3]With the KamLAND results in the earlier versions of [10] which did not include the new background, the best-fit values were $\Delta m^2_{21} = 8.4 \times 10^{-5}$ eV^2, $\sin^2\theta_{12} = 0.24$ and $\chi^2_{min}/d.o.f. = 19.46/10$. Thus, the inclusion of the new background in our analysis is seen to have changed the best-fit oscillation parameters as well as improved the goodness of fit (g.o.f). This is in agreement with what the KamLAND collaboration has obtained.

Data set used	(3σ)Range of Δm^2_{21} eV^2	(3σ)spread in Δm^2_{21}	(3σ) Range of $\sin^2\theta_{12}$	(3σ) spread in $\sin^2\theta_{12}$
only sol	3.0 - 17.0	70%	$0.21 - 0.39$	30%
sol+162 Ty KL	4.9 - 10.7	37%	$0.21 - 0.39$	30%
sol+ 766.3 Ty KL	7.0 - 9.4	15%	$0.21 - 0.38$	29%

Table 1: 3σ allowed ranges of Δm^2_{21} and $\sin^2\theta_{12}$ from the analysis of the global solar neutrino, and global solar neutrino + KamLAND (past and present) data. We show also the % spread in the allowed values of the two neutrino oscillation parameters.

theoretical errors. The ^8B flux normalisation factor f_B is left to vary freely in the analysis. For the other solar neutrino fluxes (pp, pep, ^7Be, CNO, hep), the predictions and estimated uncertainties of the most recent standard solar model (SSM) [23] (BP04) have been utilized. For further details of our solar neutrino data analysis we refer the reader to our earlier papers [13, 15, 18].

We find that with the inclusion of the latest KamLAND spectrum data, the high-LMA region is disfavored at more than 99.9% C.L. in a 2 parameter fit. Thus, the high-LMA solution is excluded at more than 3σ. This establishes the low-LMA solution as unique solution of the solar neutrino problem. It also confirms our prediction [18] that, if the best-fit of the KamLAND spectrum data corresponds to a point in the low-LMA solution region, there will be no high-LMA region allowed at 3σ level. The best-fit point we get from the combined solar neutrino and KamLAND data analysis is,

$$\Delta m^2_{21} = 8.0 \times 10^{-5}\ \text{eV}^2, \quad \sin^2\theta_{12} = 0.28, \quad \text{f}_\text{B} = 0.88, \quad \chi^2_\text{min}/\text{d.o.f.} = 85.42/92 \tag{5}$$

in good agreement with that obtained in [10]. Note that the best-fit point from the global solar neutrino data analysis,

$$\Delta m^2_{21} \ = 6.07 \times 10^{-5}\ \text{eV}^2, \quad \sin^2\theta_{12} = 0.29, \quad \text{f}_\text{B} = 0.90, \quad \chi^2_\text{min}/\text{d.o.f.} = 69.06/80 \tag{6}$$

lies outside the 3σ range, allowed after including the new KamLAND data. However, the χ^2 function for the solar neutrino data changes weakly when Δm^2_{21} varies in an interval of values which is centered on the best fit value in eq. (6) and includes the best fit value of the global data set, eq. (5) (see Fig. 3). The best-fit value of Δm^2_{21} in the global fit is controlled by the KamLAND data, whereas the best-fit value of $\sin^2\theta_{12}$ is controlled by the global solar neutrino data. The Δm^2_{21} allowed region is seen to have narrowed down considerably making it possible to plot it on a linear scale.

In Table 1 we present the 3σ allowed ranges of Δm^2_{21} and $\sin^2\theta_{12}$, obtained using different data sets. We also show the uncertainty in the value of the parameters through a quantity "spread" which we define as

$$\text{spread} = \frac{prm_{max} - prm_{min}}{prm_{max} + prm_{min}} \times 100, \tag{7}$$

where prm denotes the parameter Δm^2_{21} or $\sin^2\theta_{12}$, and prm_{max} and prm_{min} are the maximal and minimal values of the chosen parameter allowed at a given C.L. Table 1 illustrates the remarkable sensitivity of the KamLAND experiment to Δm^2_{21}, which results in stringent constraints on the allowed values of Δm^2_{21}. However, the KamLAND experiment does not constrain the allowed range of θ_{12} much better than the solar neutrino experiments.

So far we have given the allowed regions of Δm^2_{21} and $\sin^2\theta_{12}$, obtained from the two parameter fits of the data. It is instructive to see the bounds on the oscillation parameters using one parameter plots of $\Delta\chi^2 = \chi^2 - \chi^2_{min}$ vs. Δm^2_{21} and vs. $\sin^2\theta_{12}$. In Fig. 3 we show the dependence of $\Delta\chi^2$ on $\sin^2\theta_{12}$ (left hand panel) and on Δm^2_{21} (right hand panel) after marginalising over the remaining free parameters. In this analysis only the solar neutrino data, and the solar neutrino + 766.3 Ty KamLAND spectrum data have been used. We find that the allowed range of Δm^2_{21} values becomes much narrower compared to that obtained using only the global solar neutrino data. The inclusion of the recent KamLAND results makes the $\Delta\chi^2$ for the high-LMA region even larger, excluding it at more than 4σ for a one parameter fit. From this figure we also see that the best-fit value of Δm^2_{21} , obtained from the global solar neutrino data, has a $\Delta\chi^2 > 40$, and hence is disfavored at $> 6\sigma$. The inclusion of the new KamLAND spectrum data disfavors maximal solar neutrino mixing to a greater degree. The $\Delta\chi^2$ value at $\sin^2\theta_{12} = 0.5$ is a little above 40, thereby excluding the maximal mixing at more than 6σ for a one parameter fit. Figure 3, showing the dependence of $\Delta\chi^2$ on $\sin^2\theta_{12}$, corroborates our results presented in Table 1, namely, that the allowed range of $\sin^2\theta_{12}$ does not change considerably up to the 3σ level with the inclusion of the new KamLAND results. The reason for this can be traced to the fact that for the values of Δm^2_{21} and $\sin^2\theta_{12}$ allowed by the combined solar neutrino and KamLAND data, the Earth matter effects are negligible at the baselines relevant for the KamLAND experiment and the relevant $\bar{\nu}_e$ survival probability reads:

$$P^{KL}_{ee} \approx 1 - \sin^2 2\theta_{12} \sin^2\left(\frac{\pi L}{\lambda}\right), \tag{8}$$

where λ denotes the oscillation length,

$$\lambda = 2.47 \ \frac{\mathrm{eV}^2}{\Delta m^2} \frac{E}{\mathrm{MeV}} \ m. \tag{9}$$

On the other hand, if we neglect the Earth matter effects in the solar neutrino transitions, which are rather small, the ν_e survival probability relevant for the interpretation of the data of the SNO and SK solar neutrino experiments, is given by the adiabatic MSW prediction [12]

$$P^{sno}_{ee} \approx \sin^2\theta_{12}. \tag{10}$$

Since $\sin^2 2\theta_{12}$ is a less sensitive function of θ_{12} compared to $\sin^2\theta_{12}$, the survival probability relevant for the interpretation of the KamLAND data is less sensitive to θ_{12} than that measured at SNO. Moreover, the average e^+- energy measured at KamLAND (~ 5 MeV), and the average source-detector distance for KamLAND (~ 180 km), correspond to $L \sim \lambda$ for the best-fit Δm^2_{21}. At $L \sim \lambda$, the $\bar{\nu}_e$ survival probability has a maximum (SPMAX). This means that the coefficient of the $\sin^2 2\theta_{12}$ term in P^{KL}_{ee} is relatively small, preventing the KamLAND experiment to reach

Experiment	Observed rate/BP04 prediction	Predicted Rate at global best-fit	Predicted Rate at solar best-fit
Ga	0.52 ± 0.029	0.546	0.538
Cl	0.301 ± 0.027	0.350	0.346
SK(ES)	0.406 ± 0.014	0.395	0.396
SNO(CC)	0.274 ± 0.019	0.291	0.290
SNO(ES)	0.38 ± 0.052	0.387	0.387
SNO(NC)	0.895 ± 0.08	0.879	0.903

Table 2: The observed rates w.r.t predictions from the latest Standard Solar Model [23]. We also show the predicted rates for the best fit values of Δm^2_{21} and $\sin^2\theta_{12}$, obtained in the analysis of the i) global solar neutrino data, and ii) global solar neutrino +KamLAND data.

high precision in the determination of θ_{12}. Evidently, the sensitivity to θ_{12} can be improved by reducing the baseline length to $L \sim \lambda/2$, corresponding to a minimum of the $\bar{\nu}_e$ survival probability (SPMIN) [24]. We shall come back to this point later.

3 Consistency Check between Different Experiments

In this Section we check the consistency between the allowed regions obtained using data from different experiments. In Fig. 4 we compare the KamLAND spectrum data with the predictions for the spectrum obtained for values of Δm^2_{21} and $\sin^2\theta_{12}$ corresponding to the i) solar neutrino data best-fit point, ii) KamLAND spectrum data best-fit point, and iii) solar neutrino +KamLAND spectrum data best-fit point. We also show the unoscillated spectrum obtained by us. This agrees fairly well with that given by the KamLAND collaboration in [10] indicating that we have correctly implemented the reactor power and operation schedules from the availbale sources. This figure clearly illustrates the sensitivity of the predicted spectrum to Δm^2_{21}, and the deviations of the observed spectrum from that predicted at the solar neutrino data best-fit point. In the absence of the KamLAND results, it was necessary to compare the "low" and "high" energy CC solar neutrino data to determine Δm^2_{21}, and to compare the CC and NC data to determine $\sin^2\theta_{12}$. With Δm^2_{21} determined using the new KamLAND results, one can make a consistency check by dispensing with the data from anyone of the solar neutrino experiments.

In Fig. 5 we present the allowed regions obtained by taking out the data from one solar neutrino experiment from the global data set. As before we let the ^8B flux normalisation vary freely in the analysis. The figure shows that the allowed region is robust and does not change considerably when the data from one experiment is left out of the analysis. Taking out the SNO data will lead to smaller values of f_B, and correspondingly larger values of $\sin^2\theta_{12}$ being allowed. Using the 162 Ty KamLAND data and taking out the SNO results from the analysis, made the maximal mixing solution allowed [25]. With the 766.3 Ty KamLAND data included in the analysis, the maximal mixing is ruled out at 3σ even leaving out the SNO data from the data set used in the analysis. This

is a consequence of the increased precision of the KamLAND data which disfavours the maximal mixing solution. In Table 2 we compare the observed event rates in the different solar neutrino experiments with those predicted for the best fit values of Δm^2_{21} and $\sin^2\theta_{12}$, obtained in the analysis of the global solar neutrino data and global solar neutrino + KamLAND spectrum data. Note that the SNO NC event rate relative to the SSM prediction of BP04 is $f_B = 0.895 \pm 0.08$, while its earlier central value, with respect to the SSM prediction of BP00, was slightly above 1. This drop simply reflects the increase in the central value of the ^8B flux from 5.1×10^{-5} cm$^{-2}s^{-1}$ to 5.8×10^{-5} cm$^{-2}s^{-1}$ in the latest SSM of BP04 [23]. There is a corresponding drop in the other experimental rates shown in Table 2. However, this renormalisation has no effect on our results since we have not used SSM prediction for the normalisation of the ^8B flux. Instead we have left f_B as a free parameter to be determined by the solar neutrino data. This parameter is primarily determined by the NC event rate measured in SNO. We see from Table 2 that all the measured event rates, except that observed in the Cl experiment, are in very good agreement with the predicted ones. There is very little difference between the predictions, corresponding to the solar neutrino data and solar neutrino + KamLAND spectrum data best-fit points. This shows the insensitivity of the fit of the solar neutrino data to small variations in Δm^2, in contrast to the fit of the KamLAND spectrum data. Note that the obtained Cl rate is by 2σ lower than the global best-fit prediction. This is a statistically small but well known deviation which cannot be explained by the LMA solution [26]. If such a deviation is confirmed by future intermediate energy solar neutrino experiments like Borexino, it will call for some additional subdominant mechanism of solar neutrino transitions.

4 Three Flavour Neutrino Mixing Analysis

In this Section we present results obtained from the analysis of the global data on solar and reactor neutrinos within a three-flavor neutrino mixing framework. In this case $\Delta m^2_{21} \cong \Delta m^2_{\odot}$ and $\Delta m^2_{31} \cong \Delta m^2_{atm}$. The best-fit value of Δm^2_{atm}, obtained in the latest two-neutrino mixing analysis of the Super-Kamiokande atmospheric neutrino data on the Zenith-angle distribution of the $\mu-$like events is 2.1×10^{-3} eV^2 [27]. Thus, the two-neutrino mixing analyses of the solar and atmospheric neutrino data indicate that $\Delta m^2_{21} << \Delta m^2_{31}$. Under this approximation the effect of the third heaviest neutrino in the relevant solar neutrino and reactor anti-neutrino survival probabilities is due mainly to the mixing angle θ_{13}. The relevant ν_e and $\bar{\nu}_e$ survival probabilities in the three-neutrino mixing cases of interest are given by the following expression:

$$P^{3\nu}_{ee} \cong \cos^4\theta_{13} P^{2\nu}_{ee} + \sin^4\theta_{13}, \tag{11}$$

where $P^{2\nu}_{ee}$ is the ν_e or $\bar{\nu}_e$ survival probability in the case of two-neutrino mixing (see, e.g., [29]). For solar neutrinos, $P^{2\nu}_{ee} \equiv P^{2\nu}_{ee\odot}$ is the two-neutrino mixing ν_e survival probability [30] with the solar electron number density N_e replaced by $N_e\cos^2\theta_{13}$. In the case of KamLAND experiment one has $P^{2\nu}_{ee} \equiv P^{2\nu}_{eeKL}$, where $P^{2\nu}_{eeKL}$ is given by eq. (8) in which $\Delta m^2 \equiv \Delta m^2_{21}$.

Strong constraints on the value of θ_{13} have been obtained in the CHOOZ and Palo Verde reactor antineutrino experiments [28]. We include the CHOOZ results in our three-flavour neutrino

mixing analysis (see also [31]). In the limit of $\Delta m^2_{21} << \Delta m^2_{31}$, the probability relevant for the interpretation of the CHOOZ data is given by

$$P^{3\nu}_{eeCHOOZ} \cong 1 - \sin^2 2\theta_{13} \sin^2(\Delta m^2_{31} L/4E). \tag{12}$$

We note that $P^{3\nu}_{eeCHOOZ}$ depends on Δm^2_{31}, while $P^{2\nu}_{ee\odot}$ and $P^{2\nu}_{eeKL}$ depend on Δm^2_{21}.

We allow Δm^2_{31} to vary freely within the 3σ range $(1.28 - 4.17) \times 10^{-3}$ eV^2, obtained using the one parameter $\Delta\chi^2$ vs Δm^2_{31} fit of the SK atmospheric neutrino Zenith angle data, presented by the SK Collaboration at the Neutrino 2004 International Conference [27] [4], and perform a combined three-neutrino oscillation analysis of the global solar neutrino and reactor anti-neutrino data, including both the KamLAND and CHOOZ results. The best-fit values of the parameters obtained from the three-flavor neutrino mixing analysis are:

$$\Delta m^2_{21} = 8.0{\times}10^{-5}\,\mathrm{eV}^2,\ \ \sin^2\theta_{12} = 0.28,\ \ \sin^2\theta_{13} = 0.004,\ \ f_B = 0.88,\ \ \chi^2_{min}/d.o.f. = 91.68/105 \tag{13}$$

In Fig. 6 we present the $\Delta\chi^2$ as a function of $\sin^2\theta_{13}$, for Δm^2_{31} allowed to vary within its 3σ allowed range [27], $(1.28 - 4.17) \times 10^{-3}$ eV^2, and the other parameters allowed to vary freely. The 3σ bounds on $\sin^2\theta_{13}$, obtained from CHOOZ data analysis, can be directly read from the figure for a one parameter fit as $\sin^2\theta_{13} < 0.07$. The bound derived from the combined analysis of the solar neutrino, CHOOZ and KamLAND data is $\sin^2\theta_{13} < 0.055$.

In Fig. 7 we show the allowed regions in the Δm^2_{21} $-\sin^2\theta_{12}$ plane for four fixed values of θ_{13}. We note that although the presence of a small non-zero θ_{13} can improve the fit in the regions of the parameter space with higher values of Δm^2_{21} [18], i.e., in the high-LMA zone, the new KamLAND data are able to exclude the high-LMA region at more than 3σ even in the presence of a third generation in the mixing, indicating the robustness of the low-LMA solution.

5 Future Projections

The recent KamLAND data combined with the solar neutrino data unambiguously determine the low-LMA solution as unique solution of the solar neutrino problem. It also enables us to determine Δm^2_{21} with a relatively high precision: $\sim 10\%$ at 90% C.L. The high-LMA solution is disfavored at more than 3σ. The uncertainty in the value of Δm^2_{21} is expected to diminish further as KamLAND collects more data. However, as we have stressed before, the KamLAND experiment does not appreciably reduce the error on the value of $\sin^2\theta_{12}$ [24].

In the near future, the SNO collaboration is expected to publish data on the CC (e^-) day/night spectrum, observed during the salt phase of the experiment. The recent KamLAND results allow us to make relatively precise predictions for the the day-night asymmetry in the SNO experiment:

$$A_{DN} = 2\frac{N - D}{N + D}. \tag{14}$$

[4] The allowed range of θ_{13} depends crucially on the allowed range of the atmospheric mass squared difference Δm^2_{31} [25].

In the right hand panel of Fig. 8 we show the lines of constant A_{DN} values in the Δm^2_{21} $-\sin^2\theta_{12}$ plane for the SNO experiment (see also, e.g., [32, 33]). The predicted A_{DN} in SNO for the current best-fit values of the parameters and the corresponding 3σ range, are given by:

$$A_{DN}(SNO) = 0.034, \quad 3\sigma \text{ range}: \ 0.027 - 0.043. \tag{15}$$

The published SNO result on the D/N asymmetry is $A^{exp}_{DN}(SNO) = 7 \pm 5\%$. Thus, the error has to be reduced to $\sim 1\%$ in order to observe $A_{DN}(SNO) \neq 0$ at $\sim 3\sigma$ level.

In the left hand panel of the same figure we also plot the iso-CC/NC contours for SNO. The measured value of the CC to NC ratio from the salt phase of SNO experiment is,

$$R^{salt}_{CC/NC} = 0.305 \pm 0.033. \tag{16}$$

The phase III of SNO will collect neutral current data using Helium counters [34]. This would give a totally uncorrelated information on the CC and NC event rates observed in SNO and a reduced error for the NC event rate. The projected total error for the observed NC event rate for this phase is 6% [34]. For the CC event rate we assume that the statistical error during the phase III would be approximately the same as in each of the earlier two phases, while the systematic error is taken to be 4.5%, i.e., slightly smaller than the 5% reported in phases I and II of SNO. Thus, we assume that the total error in CC event rate measurement from all the three phases combined will be about 5%. If the central value of the CC and NC event rate ratio would remain the same as observed in the salt phase, the CC/NC ratio expected to be measured in the phase III of the SNO experiment would be

$$R^{He}_{CC/NC} = 0.305 \pm 0.024. \tag{17}$$

Since for $\Delta m^2_{21} \lesssim 10^{-4}$ eV^2 the CC/NC ratio in SNO is mainly related to the solar neutrino mixing angle (see, e.g., ref. [33], eq. (10) and the left hand panel in Fig. 8), the reduction in the $R_{CC/NC}$ error is expected to result in an improvement in the precision of $\sin^2\theta_{12}$ determination. We have made a projected analysis of the global solar neutrino data, including the upgraded CC and NC errors expected from the phase III of the SNO experiment. The range of allowed values of $\sin^2\theta_{12}$ could be reduced to about $0.22 - 0.34$ $(0.21 - 0.36)$ at 99% C.L. (99.73% C.L.), corresponding to a spread of 21% (26%) [35].

There has been a recent proposal of adding 0.1% gadolinium to the water in the Super-Kamiokande detector to improve the detector sensitivity to neutrons [36]. This would result in a remarkable increase in the detector sensitivity to low energy $\bar{\nu}_e$, transforming SK into a huge reactor antineutrino detector (SK-Gd), with an event rate that is about 43 times larger than that observed in KamLAND [36, 35]. After 5 years of data taking, the SK-Gd experiment can measure Δm^2_{21} with $\sim 1\%$ and $\sin^2\theta_{12}$ with $\sim 15\%$ uncertainty at 99% C.L. [35].

As discussed earlier, a very precise measurement of $\sin^2\theta_{12}$ can be achieved in a reactor experiment with a baseline corresponding to an SPMIN of the $\bar{\nu}_e$ survival probability [24]. The condition for SPMIN is $L \cong \lambda/2 = 1.24(\mathrm{E/MeV})(\mathrm{eV^2}/\Delta \mathrm{m^2_{12}})$ m. For the low-LMA solution region and the average energy of the e^+ observed in the KamLAND experiment, this corresponds to a distance of approximately (50 - 70) km [24]. For an experiment with a 70 km baseline and 24.3 GW (18.6

GW) reactor power, corresponding to the Kashiwazaki (Daya Bay) complex in Japan (China), $\sin^2\theta_{12}$ can be determined with a $\sim 10\%$ error at 99% C.L. with a 3 kTy (4 kTy) statistics [24].

The forthcoming solar neutrino experiments are Borexino [37] and KamLAND-^7Be, which will provide an accurate measurement of the ^7Be neutrino flux, and the Low energy solar Neutrino (LowNu) experiments [39, 38], which are designed to measure the flux of solar pp neutrinos. The potential of Borexino and any generic LowNu experiment [40] in constraining the solar neutrino oscillation parameters have been studied recently in [24, 41]. For the allowed regions obtained in this paper, we find the predicted rates for Borexino and LowNu experiments to be

$$R_{Be} = 0.67, \quad (3\sigma \text{ range}: \ 0.62 - 0.72) \tag{18}$$

$$R_{pp} = 0.71, \quad (3\sigma \text{ range}: \ 0.67 - 0.76). \tag{19}$$

6 Conclusions

We have investigated the implications of including the recent KamLAND spectrum data in global solar neutrino oscillation analysis. The observed spectral distortion in the KamLAND experiment firmly establishes Δm^2_{21} to lie in the low-LMA solution region. The high-LMA solution is excluded at more than 4σ by the global solar neutrino and KamLAND spectrum data. The maximal solar neutrino mixing is ruled out at 6σ level. We have found that the 3σ allowed region in the $\Delta m^2_{21} - \sin^2\theta_{12}$ plane remains remarkably stable even when we leave out the data from one of the solar neutrino experiments from the global fit. Likewise, there is practically no increase in the allowed region when one goes from two to three flavor neutrino oscillation analysis of the global solar neutrino and KamLAND spectrum data. The 3σ upper limit on $\sin^2\theta_{13}$ was found to be $\sin^2\theta_{13} < 0.055$. We have derived predictions for the CC to NC event rate ratio and day-night (D-N) asymmetry in the CC event rate, measured in the SNO experiment, and for the suppression of the event rate in the BOREXINO and LowNu experiments, designed to measure the ^7Be and pp solar neutrino fluxes. With the value of Δm^2_{21} determined more precisely using the current solar neutrino and KamLAND data, the predicted range of possible values of the day-night asymmetry in the CC event rate at SNO narrows down to (0.025 - 0.041) at 99.73% C.L. Remarkably high precision in the measurement of Δm^2_{21} can be achieved with the Super-Kamiokande detector loaded with 1% gadolinium: this would transform Super-Kamiokande into a huge reactor $\bar{\nu}_e$ detector (SK-Gd) with an event rate 43 times larger than that observed in the KamLAND experiment. Finally, we have discussed how the precision of $\sin^2\theta_{12}$ determination can improve with the increasing of the precision of the future SNO data, by the SK-Gd reactor $\bar{\nu}_e$ oscillation experiment, as well as, by performing a reactor $\bar{\nu}_e$ oscillation experiment with a baseline of ~ 70 km.

With the publication of the latest KamLAND data the neutrino oscillation origin of the observed solar neutrino deficit is firmly established. The future high precision measurements of the solar neutrino oscillation parameters will be of fundamental importance for understanding the true origin of the flavour neutrino mixing.

S.G. and D.P.R. would like to thank respectively SISSA and The Abdus Salam International Centre for Theoretical Physics for hospitality. This work was supported by the Italian INFN under the program "Fisica Astroparticellare" (S.T.P.).

References

[1] B. T. Cleveland *et al.*, Astrophys. J. **496**, 505 (1998).

[2] B. Pontecorvo, Chalk River Lab. report PD–205, 1946.

[3] Y. Suzuki, Nucl. Phys. Proc. Suppl. **38** (1995) 54.

[4] J. N. Abdurashitov *et al.* [SAGE Collaboration], J. Exp. Theor. Phys. **95**, 181 (2002) [Zh. Eksp. Teor. Fiz. **122**, 211 (2002)] [arXiv:astro-ph/0204245]; W. Hampel *et al.* [GALLEX Collaboration], Phys. Lett. B **447**, 127 (1999); C. Cattadori, Talk at Neutrino 2004, Paris, France, June 14-19, 2004.

[5] S. Fukuda *et al.* [Super-Kamiokande Collaboration], Phys. Lett. B **539**, 179 (2002) [arXiv:hep-ex/0205075].

[6] Q. R. Ahmad *et al.* [SNO Collaboration], Phys. Rev. Lett. **87**, 071301 (2001) [arXiv:nucl-ex/0106015].

[7] Q. R. Ahmad *et al.* [SNO Collaboration], Phys. Rev. Lett. **89**, 011301 (2002) [arXiv:nucl-ex/0204008]; Q. R. Ahmad *et al.* [SNO Collaboration], Phys. Rev. Lett. **89**, 011302 (2002) [arXiv:nucl-ex/0204009].

[8] S. N. Ahmed *et al.* [SNO Collaboration], arXiv:nucl-ex/0309004.

[9] K. Eguchi *et al.* [KamLAND Collaboration], Phys. Rev. Lett. **90**, 021802 (2003) [arXiv:hep-ex/0212021].

[10] T. Araki *et al.* [KamLAND Collaboration], arXiv:hep-ex/0406035 version 3.

[11] B. Pontecorvo, *Zh. Eksp. Teor. Fiz.* **33** (1957) 549 and **34** (1958) 247; *Zh. Eksp. Teor. Fiz.* **53** (1967) 1717.

[12] L. Wolfenstein, Phys. Rev. D **17**, 2369 (1978) ; S. P. Mikheev and A. Y. Smirnov, Sov. J. Nucl. Phys. **42** (1985) 913 [Yad. Fiz. **42**, 1441 (1985)].

[13] A. Bandyopadhyay, S. Choubey, S. Goswami and K. Kar, Phys. Lett. B **519**, 83 (2001) [arXiv:hep-ph/0106264].

[14] G.L. Fogli, E. Lisi, D. Montanino, A. Palazzo, Phys. Rev. **D64**, 093007 (2001); J.N. Bahcall, M.C. Gonzalez-Garcia, C. Pana-Garay, JHEP **0108**, 014 (2001); P. I. Krastev and A. Y. Smirnov, Phys. Rev. D **65**, 073022 (2002) [arXiv:hep-ph/0108177]; M.V. Garzelli and C. Giunti, JHEP **0112**, 017 (2001).

[15] A. Bandyopadhyay, S. Choubey, S. Goswami and D. P. Roy, Phys. Lett. B **540**, 14 (2002) [arXiv:hep-ph/0204286]; S. Choubey, A. Bandyopadhyay, S. Goswami and D. P. Roy, arXiv:hep-ph/0209222 and references therein.

[16] A. Bandyopadhyay, S. Choubey, R. Gandhi, S. Goswami and D. P. Roy, Phys. Lett. B **559**, 121 (2003) [arXiv:hep-ph/0212146].

[17] G. L. Fogli et al., Phys. Rev. D **67**, 073002 (2003) [arXiv:hep-ph/0212127]; M. Maltoni, T. Schwetz and J. W. Valle, Phys. Rev. D **67**, 093003 (2003) [arXiv:hep-ph/0212129]; J. N. Bahcall, M. C. Gonzalez-Garcia and C. Pena-Garay, JHEP **0302**, 009 (2003) [arXiv:hep-ph/0212147]; H. Nunokawa, W. J. Teves and R. Zukanovich Funchal, Phys. Lett. B **562**, 28 (2003) [arXiv:hep-ph/0212202]; P. Aliani et al., arXiv:hep-ph/0212212; P. C. de Holanda and A. Y. Smirnov, JCAP **0302**, 001 (2003) [arXiv:hep-ph/0212270].

[18] A. Bandyopadhyay, S. Choubey, S. Goswami, S. T. Petcov and D. P. Roy, Phys. Lett. B **583**, 134 (2004) [arXiv:hep-ph/0309174].

[19] G. L. Fogli, E. Lisi, A. Marrone and A. Palazzo, Phys. Lett. B **583**, 149 (2004) [arXiv:hep-ph/0309100]. P. C. de Holanda and A. Y. Smirnov, Astropart. Phys. **21**, 287 (2004) [arXiv:hep-ph/0309299].

[20] A. Bandyopadhyay, S. Choubey, R. Gandhi, S. Goswami and D. P. Roy, J. Phys. G **29**, 2465 (2003) [arXiv:hep-ph/0211266].

[21] G.A. Horton-Smith, talk at Neutrino Oscillations in Venice, December 3-5, 2003, Venice, Italy; *http://axpd24.pd.infn.it/NO-VE/NO-VE.html*

[22] http : //www.fepc − atomic.jp/public$_{\rm i}$nfo/public/index.html.

[23] J. N. Bahcall and M. H. Pinsonneault, Phys. Rev. Lett. **92**, 121301 (2004) [arXiv:astro-ph/0402114].

[24] A. Bandyopadhyay, S. Choubey and S. Goswami, Phys. Rev. D **67**, 113011 (2003) [arXiv:hep-ph/0302243].

[25] S. Goswami, talk at Neutrino 2004, Paris, *http://neutrino2004.in2p3.fr*

[26] S. Choubey, S. Goswami and D. P. Roy, Phys. Rev. D **65** (2002) 073001 [arXiv:hep-ph/0109017]; S. Choubey, S. Goswami, N. Gupta and D. P. Roy, Phys. Rev. D **64** (2001) 053002 [arXiv:hep-ph/0103318].

[27] E. Kearns, talk at Neutrino 2004, Paris, http://neutrino2004.in2p3.fr.

[28] M. Apollonio *et al.*, *Phys. Lett.* **B466** (1999) 415; F. Boehm *et al.*, *Phys. Rev.* **D62** (2000) 072002.

[29] S.T. Petcov, Phys. Lett. B **214**, 259 (1988).

[30] S.T. Petcov, Phys. Lett. B **200**, 373 (1988), and Phys. Lett. B **214**, 139 (1988); S.T. Petcov and J. Rich, Phys. Lett. B **224**, 401 (1989); P.I. Krastev and S.T. Petcov, Phys. Lett. B **207**, 64 (1988); E. Lisi et al., Phys. Rev. D **63**, 093002 (2000).

[31] S.M. Bilenky, D. Nicolo and S.T. Petcov, *Phys. Lett.* **B538** (2002) 77.

[32] M. Maris and S. T. Petcov, Phys. Rev. D **62** (2000) 093006 [arXiv:hep-ph/0003301].

[33] M. Maris and S. T. Petcov, Phys. Lett. B **534** (2002) 17 [arXiv:hep-ph/0201087].

[34] Kevin Graham, talk at NOON 2004, February 11-15, 2004, Tokyo, Japan, *http://www-sk.icrr.u-tokyo.ac.jp/noon2004/*; H. Robertson for the SNO Collaboration, Talk given at TAUP 2003, Univ. of Washington, Seattle, Washington, September 5 - 9, 2003, *http://mocha.phys.washington.edu/taup2003*

[35] S. Choubey and S. T. Petcov, Phys. Lett. B **594**, 333 (2004) [arXiv:hep-ph/0404103].

[36] J. F. Beacom and M. R. Vagins, arXiv:hep-ph/0309300.

[37] G. Alimonti *et al.* [Borexino Collaboration], Astropart. Phys. **16**, 205 (2002) [arXiv:hep-ex/0012030].

[38] R. S. Raghavan, Talk given at the Int. Workshop on Neutrino Oscillations and their Origin (NOON2004), February 11 - 15, 2004, Tokyo, Japan; for further information see the web-site: http://www.phys.vt.edu∼kimballton/ .

[39] M. Nakahata, Talk given at the Int. Workshop on Neutrino Oscillations and their Origin (NOON2004), February 11 - 15, 2004, Tokyo, Japan.

[40] S. Schönert,

talk at Neutrino 2002, Munich, Germany, (*http://neutrino2002.ph.tum.de*).

[41] J. N. Bahcall and C. Pena-Garay, JHEP **0311**, 004 (2003) [arXiv:hep-ph/0305159].

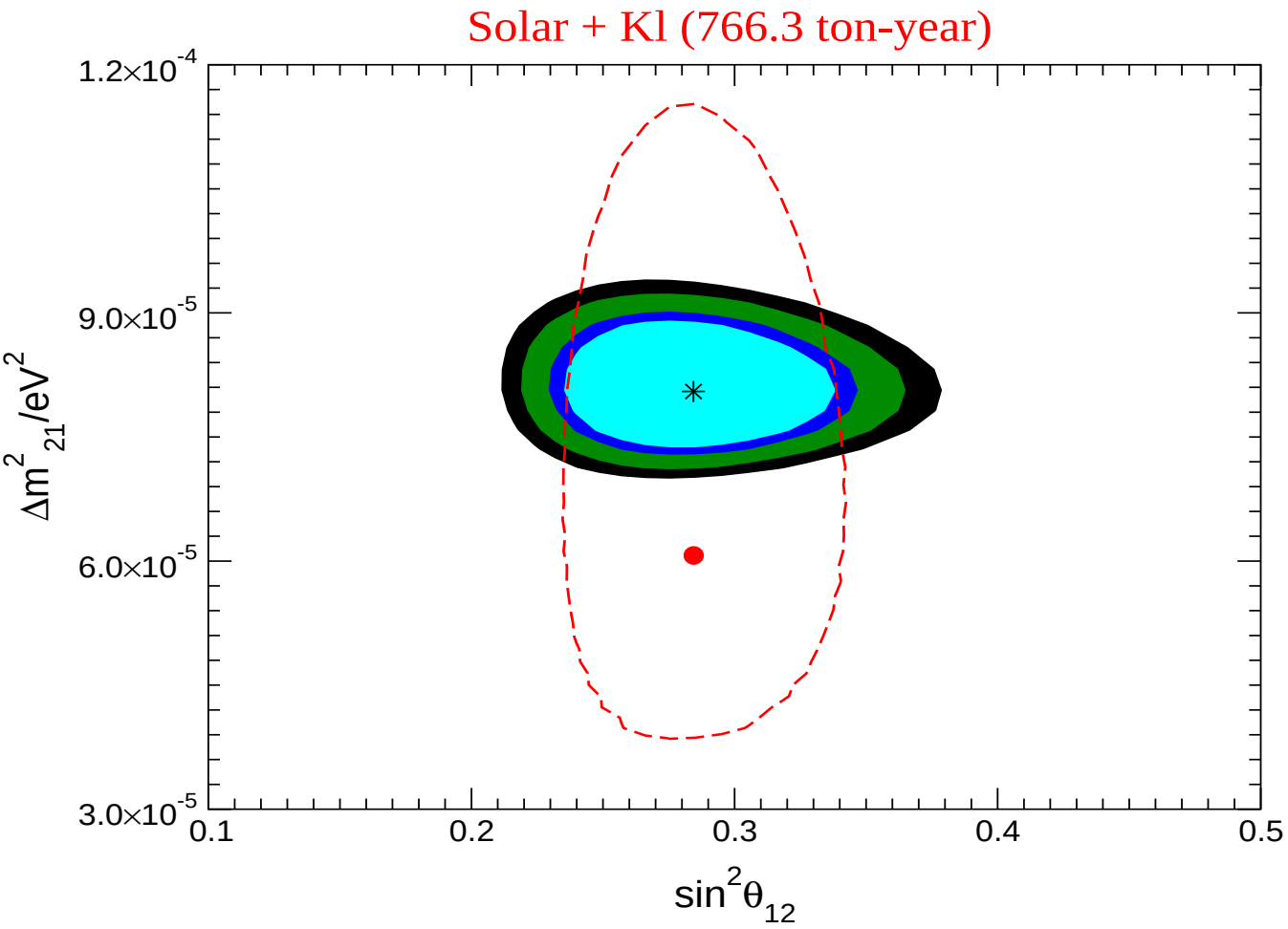

Figure 2: The 90%, 95%, 99% and 99.73% C.L. allowed regions in the Δm^2_{21} – $\sin^2\theta_{12}$ plane, obtained in a combined χ^2-analysis of the global solar neutrino and the 766.3 Ty KamLAND spectrum data (shaded areas). The region allowed by the solar neutrino data alone at 90% C.L. is also shown for comparison (region within the dashed-line contour). The best-fit points are marked in both cases.

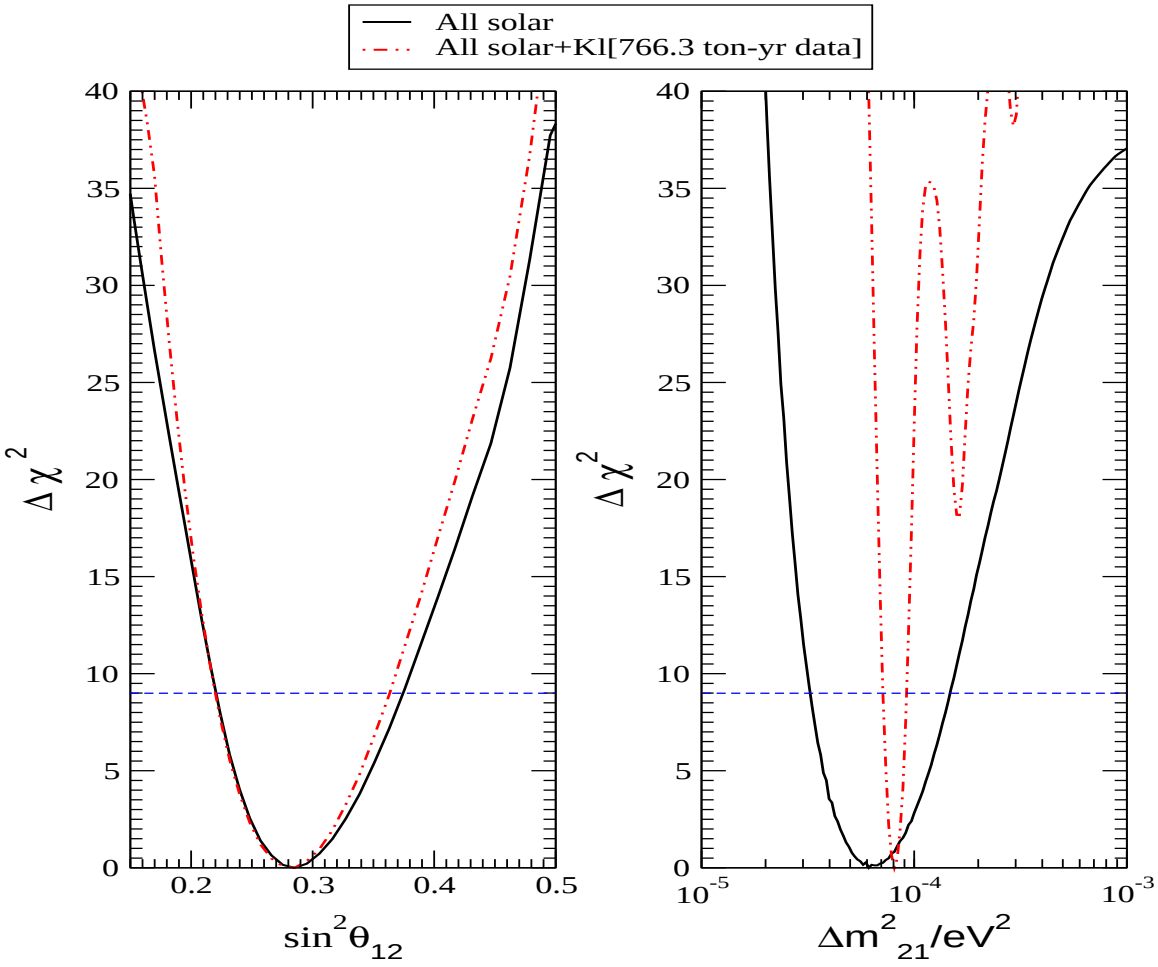

Figure 3: Bounds on Δm^2_{21} and $\sin^2\theta_{12}$ from the $\Delta\chi^2$ as a function of Δm^2_{21} and $\sin^2\theta_{12}$, respectively. The results shown in both panels are obtained by allowing all the other parameters to vary freely. The dashed line shows the 3σ limit corresponding to 1 parameter fit.

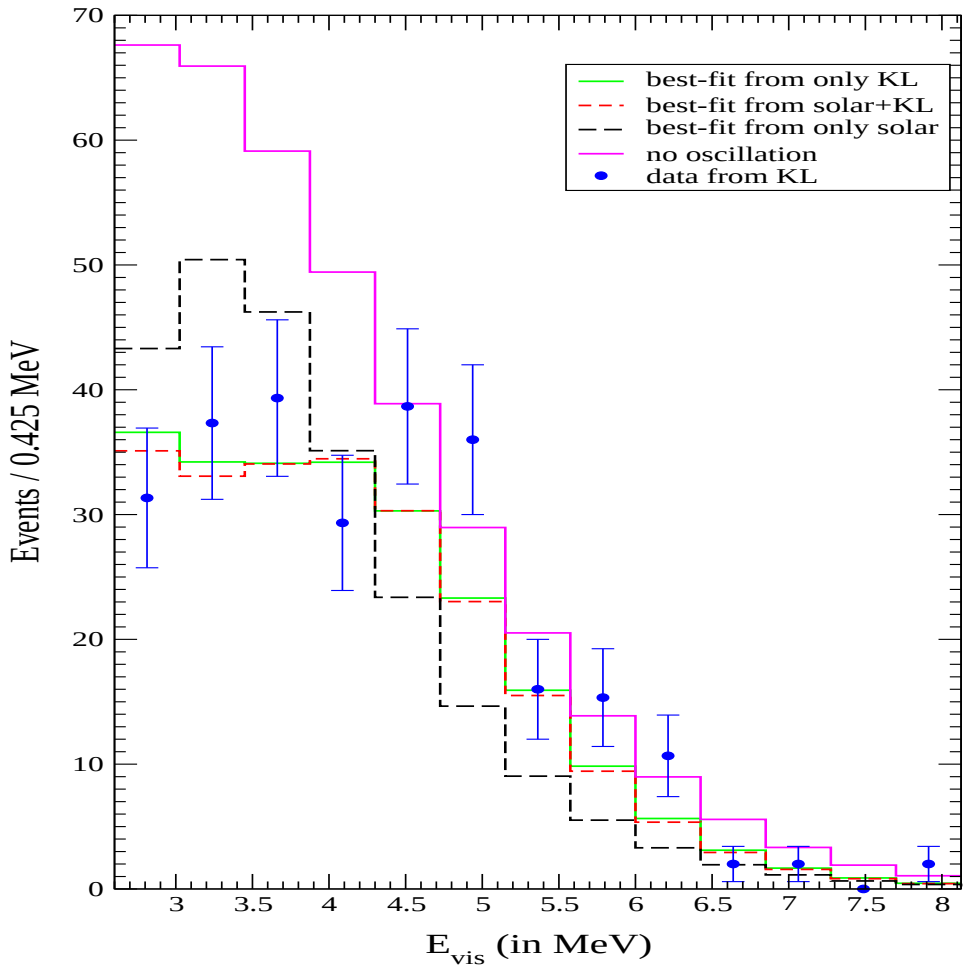

Figure 4: Predictions for the spectrum measured in the KamLAND experiment, for values of Δm^2_{21} and $\sin^2\theta_{12}$ corresponding to the i) solar neutrino data best-fit point, ii) KamLAND spectrum data best-fit point, and iii) solar neutrino +KamLAND spectrum data best-fit point. Also shown are the KamLAND 766.3 Ty spectrum data points from [10]. We also show the unoscillated spectrum obtianed by our code.

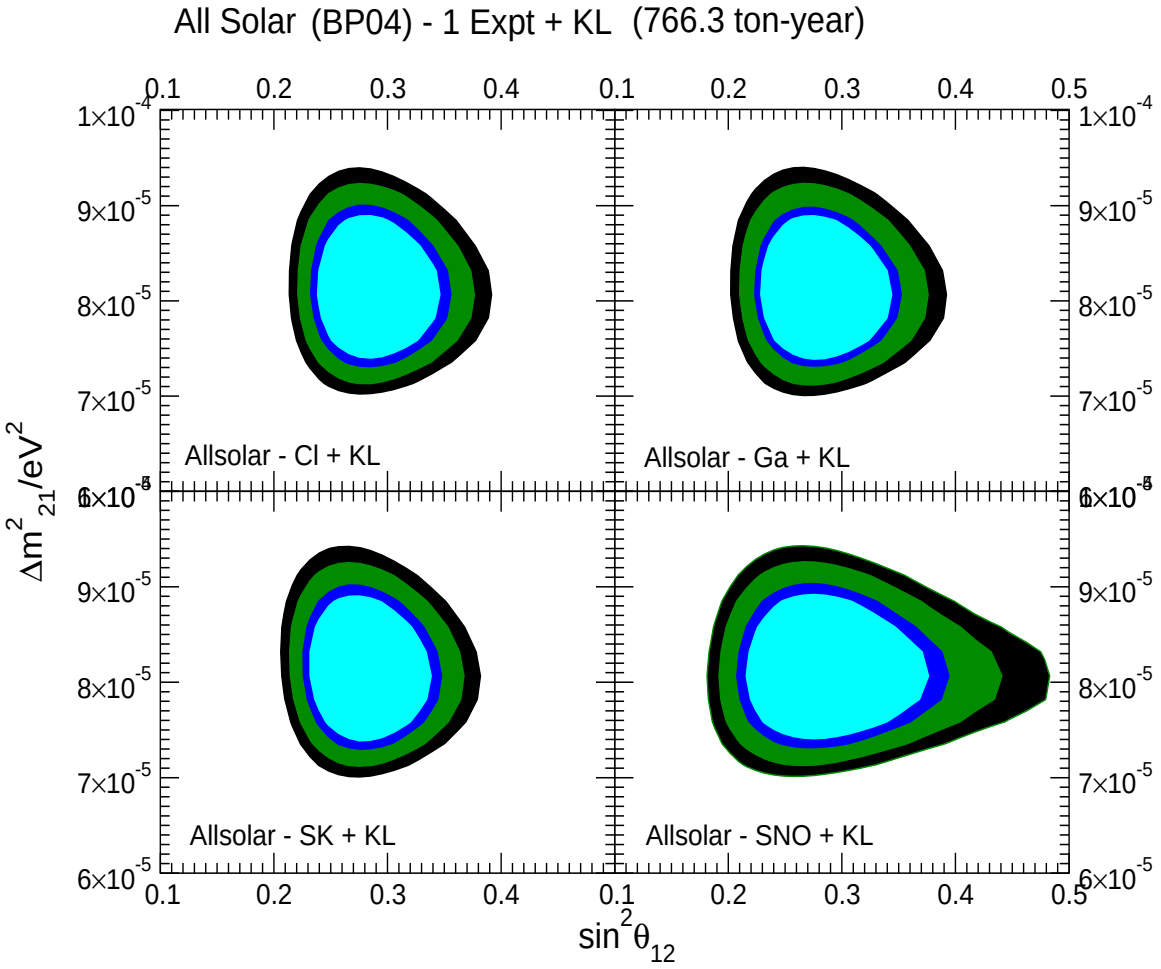

Figure 5: The allowed regions in Δm^2_{21} and $\sin^2\theta_{12}$ parameter space, obtained by removing the data from one solar neutrino experiment from the global fit.

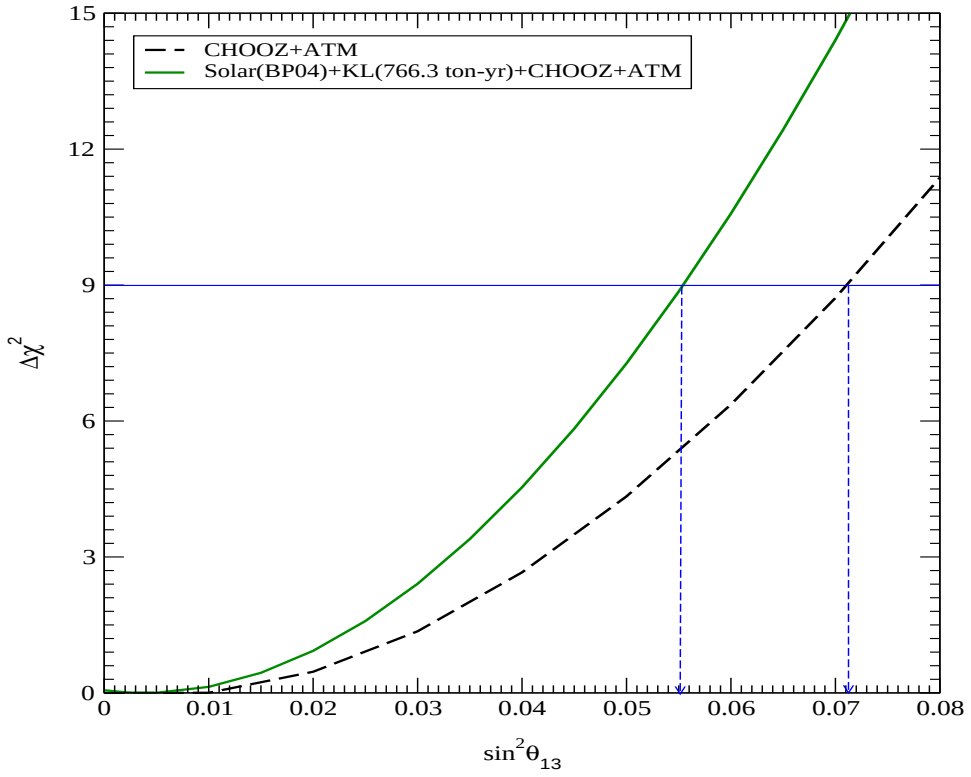

Figure 6: Bounds on the mixing angle θ_{13} from the CHOOZ data only (dashed line) and the combined solar, CHOOZ and KamLAND data (solid line). The Δm^2_{31} is allowed to vary within the 3σ range ($(1.28 - 4.17) \times 10^{-3}$ eV^2), obtained using the one parameter $\Delta\chi^2$ vs Δm^2_{31} fit of the SK atmospheric Zenith angle data, presented by the SK Collaboration in Neutrino 2004 [27]. All the other parameters are allowed to vary freely. The short-dashed lines show the 3σ limits corresponding to the case of 1 parameter fit.

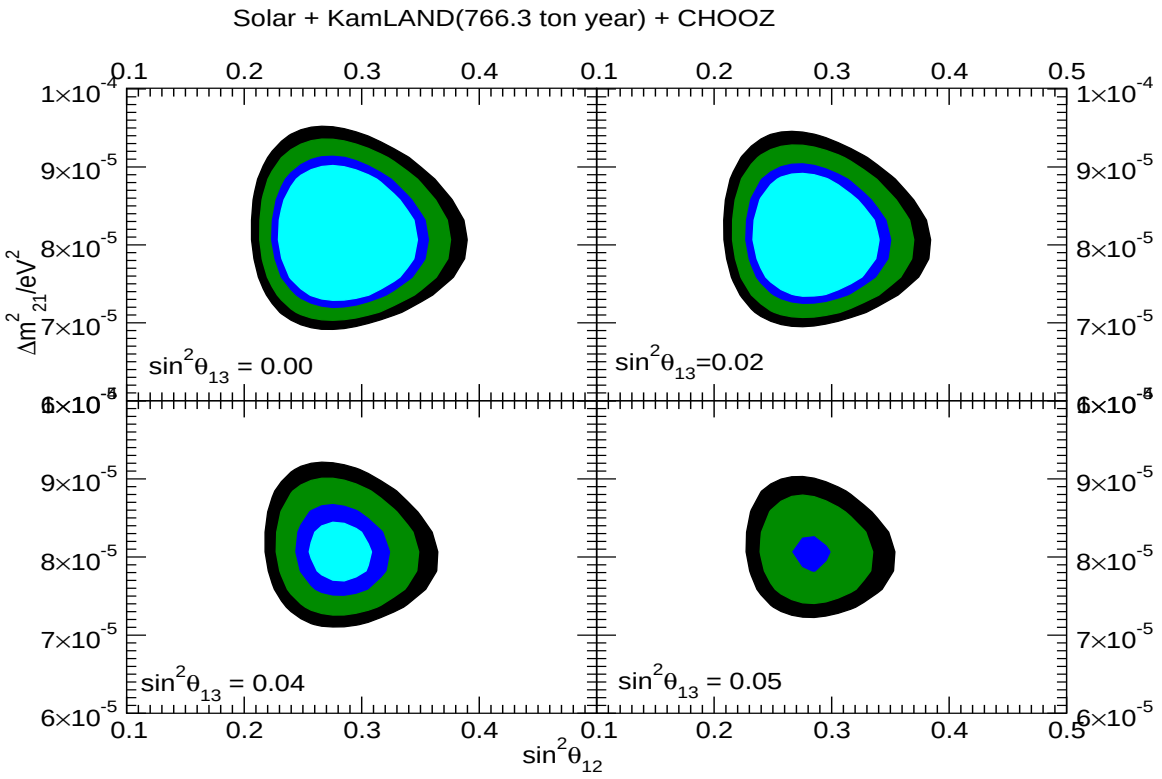

Figure 7: The 90%, 95%, 99% and 99.73% C.L. allowed regions in the Δm^2_{21} $-\sin^2\theta_{12}$ plane, obtained in a three-neutrino oscillation analysis of the global solar and reactor neutrino data, including the data from the KamLAND and CHOOZ experiments. The different panels correspond to different fixed values of $\sin^2\theta_{13}$. In the analysis Δm^2_{31} is allowed to vary freely within $(1.28 - 4.17) \times 10^{-3}$ eV^2 taken from [27]. Here we use three parameter fit $\Delta\chi^2$ values to plot the C.L. contours.

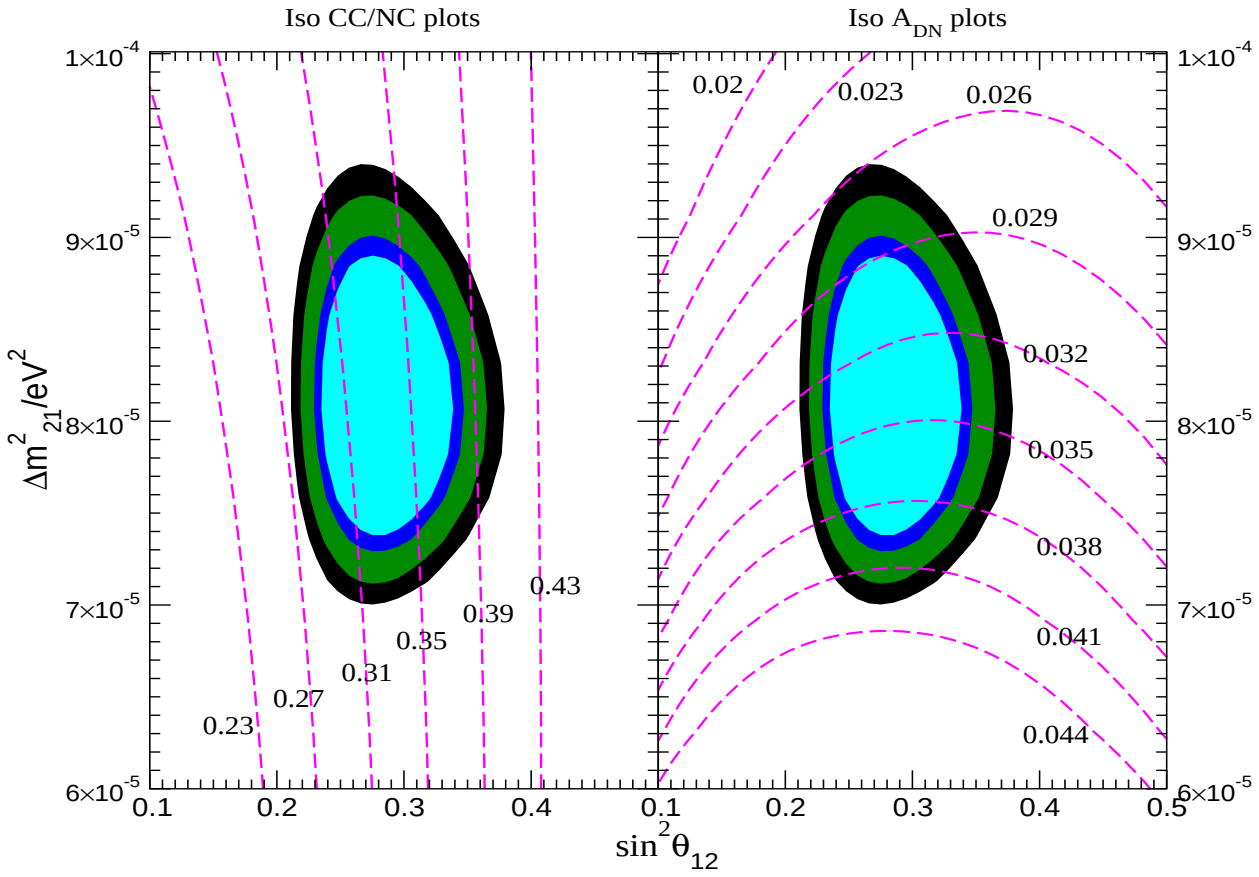

Figure 8: Lines of constant day-night asymmetry (right panel) and iso-CC/NC contours (left panel) for the SNO experiment, superposed on the allowed region obtained in the global analysis of the solar neutrino and KamLAND data.